Contents lists available at ScienceDirect

# Applied Catalysis B: Environmental

# Investigating the promotional effect of methanol on the low temperature SCR reaction on $Ag/Al_2O_3$

Sarayute Chansai [a,*], Robbie Burch [a], Christopher Hardacre [a,*], Daniel Norton [b], Xiaoying Bao [b], Larry Lewis [b]

[a] CenTACat, School of Chemistry and Chemical Engineering, Queen's University Belfast, David Keir Building, Stranmillis Road, Belfast BT9 5AG, N. Ireland, UK
[b] General Electric Global Research Center, 1 Research Circle, Niskayuna, NY 12309, USA

## ARTICLE INFO

## ABSTRACT

Methanol has been shown to promote the hydrocarbon selective catalytic reduction of $NO_x$ with octane and toluene over 2 wt% $Ag/Al_2O_3$ catalyst for the first time. In order to understand its role in the reaction fast transient kinetic methods and *in situ* DRIFTS analysis have been used. The catalytic activity tests showed that the addition of methanol to the HC-SCR reaction results in a significant improvement in the low temperature activity of a $Ag/Al_2O_3$ catalyst, despite the fact that methanol on its own is not reactive for the HC-SCR reaction. This promotional effect of methanol is dependent on the concentration of added methanol and is not necessarily associated with a higher concentration of reductant in the SCR feed. The fast transient kinetic analysis has shown that at each temperature the addition of methanol enhances the conversions of both $NO_x$ and octane and the production of $N_2$ with high selectivity in comparison with those observed with *n*-octane or toluene alone. This phenomenon is similar to the effect of $H_2$ which may be associated with the release of hydrogen and ammonia during the transient switches at 250 and 300 °C. Together with the fast transient experiments, the DRIFTS results showed that —NCO species are formed when introducing methanol to the *n*-octane-SCR feed while —CN species are removed/consumed from the surfaces of the Ag catalyst. These NCO species formed by adding methanol may play a vital role in promoting the catalytic activity of $NO_x$ reduction and methanol itself can be an *in situ* source for hydrogen formation, which subsequently enhances the SCR reaction.

## 1. Introduction

There has been extensive research on the hydrocarbon selective catalytic reduction (HC-SCR) of $NO_x$ reaction in the presence of excess oxygen with numerous catalyst formulations screened under various different reaction conditions [1–22]. One of the most promising catalysts is Ag-supported on $Al_2O_3$. However, there are a number of drawbacks with this system including the inhibitory effect of aromatics and long chain alkanes [7–9,17–22] and an insufficient $NO_x$ reduction activity in the low temperature region below 350 °C [17–22]. The latter can be mitigated to a large extent by the addition of small quantities of hydrogen (<1%) which greatly increases the low temperature activity of $Ag/\gamma-Al_2O_3$ catalysts [23–33]. Whilst only small amounts of hydrogen are present in the exhaust stream, hydrogen can be derived from the reforming

reactions, *i.e.* steam reforming and oxidative steam reforming of the fuel [34–38]. This can be undertaken on-board. Sitshebo and co-workers [38] recently studied the reduction of $NO_x$ over a full scale monolith $Ag/Al_2O_3$ catalyst from a single-cylinder diesel engine and investigated the on-board generation of hydrogen by the partial oxidation and the reforming of the exhaust gas over Rh based catalytic system. Although it was reported that hydrogen improved the efficiency of $NO_x$ reduction the reforming process must be optimized for various engine conditions in order to maximize the hydrogen production and reduce the fuel penalty. Moreover, there are difficulties regarding storage, transportation, as well as safety concerns because hydrogen is highly flammable and explosive.

There is an alternative solution in order to improve the SCR activity at low temperatures. Since the first discovery by Miyadera [39,40] that the catalytic performance of the SCR reaction over $Ag/Al_2O_3$ was significantly improved by applying oxygenated hydrocarbons, such as ethanol, propanol and acetone, the SCR of $NO_x$ reaction with these compounds has been widely studied, in particular ethanol due to the incorporation of ethanol into diesel fuel [41–44]. Shimizu et al. [45] have recently studied the

* Corresponding authors. Tel.: +44 0 28 9097 4592.
*E-mail addresses:* s.chansai@qub.ac.uk (S. Chansai), c.hardacre@qub.ac.uk (C. Hardacre).

catalytic performance of a $Ag/Al_2O_3$ catalyst for the SCR reaction (in the absence and the presence of $H_2$ and $SO_2$) with a number of oxygenated hydrocarbons (diethyl ether, ethyl tertiary butyl ether, ethanol, 1-propanol, 2-propanol, *t*-butanol, 1-propanal, ethyl acetate, and acetone). Therein, high de-$NO_x$ activity was achieved between 300 and 400 °C. Arve et al. [46] investigated the effect of bio-diesels (vegetable methyl, ethyl laurate and hexadecane) as reducing agents on the SCR reaction over $Ag/Al_2O_3$ catalyst. The use of biodiesel showed SCR activity below 400 °C, significantly higher than obtained with *n*-octane. However, this activity decreased dramatically above 400 °C. Recently, Kim et al. [47] carried out the SCR reaction over $Ag/Al_2O_3$ catalyst using simulated diesel fuel–ethanol (8.5 mol%/dodecane/7.95 mol% *m*-xylene/83.55 mol% ethanol) mixture to enhance the $NO_x$ reduction activity below 350 °C.

Engine tests have been performed using the ethanol-SCR reaction over $Ag/Al_2O_3$ [6,43,44,48]. He and Yu [6] showed that the $Ag/Al_2O_3$ exhibited $NO_x$ conversion of >80% in the temperature range of 300–400 °C. Dong et al. [43] and Zhang et al. [44] found similar results when ethanol was injected into the exhaust stream from the diesel engine. These results indicate that oxygenated hydrocarbons could be alternatives for the SCR of $NO_x$ reaction with hydrocarbons contained in the exhaust or with oxygenates added prior to the catalysts on heavy-duty vehicles by carrying on-board external tanks.

Although oxygenated hydrocarbons are reported to be very active reductants for the SCR reaction [39–46], methanol has been shown to be much less effective for the SCR reaction. Männikkö and co-workers [49,50] have recently investigated the parameters that can enhance the catalytic activity and found that a 3 wt% $Ag/Al_2O_3$ catalyst showed methanol-SCR activity over a broad range of operating temperatures between 200 and 500 °C with a maximum $NO_x$ conversion of 50% at ~300 °C [49,50].

To date, for alcohols only ethanol has been investigated in mechanistic studies [51–53] and practical applications [6,43,44,48]. We have recently discovered that methanol can enhance the HC-SCR of $NO_x$ over Ag catalysts under lean burn conditions in the absence of added $H_2$. Methanol, which can be produced from a wide range of renewable sources, has attracted attention especially for transport sector as an alternative fuel [54–59]. The methanol-blended gasoline fuels have been investigated with respect to light and heavy duty applications [59]. Moreover, methanol has been widely studied in relation to fuel cell technology as a potential innovation of our energy future and transportation system [60,61]. This could be a better solution than hydrogen fuel cell technology for fuel cell powered vehicles because methanol is inexpensive and easy to be stored and handled. Therefore, liquid methanol has several attractive features with regard to methanol-blended fuels, on-board methanol injection and methanol fuel cell for the use in transportation and methanol may overcome the disadvantages of explosive and highly flammable hydrogen gas and the complicated injection system of ammonia in the ammonia SCR technology.

The objective of this work was to improve the SCR activity, especially below 350 °C, using simulated diesel fuels (toluene or *n*-octane) by mixing the hydrocarbon with methanol. The resulting enhancement of activity was then studied to clarify the role of methanol in the reaction mechanism by using fast transient kinetics. In addition, *in situ* DRIFTS–MS analysis was used to investigate the changes in the nature of adsorbed surface species.

## 2. Experimental

### 2.1. Catalyst preparation

The $Ag/Al_2O_3$ catalyst was prepared by wetness impregnation of powdered boehmite (AlOOH, received from General Electric Global

Research) with an aqueous solution of 0.022 M $AgNO_3$. The catalyst was then filtered, dried at room temperature for 24 h and further dried at 100 °C for 3 h, after which the catalyst was calcined at 550 °C for 3 h. The Ag content of the catalyst was determined by the Inductively Coupled Plasma method to be approximately 2 wt% and the BET specific surface area of the catalyst is 225 $m^2\,g^{-1}$.

### 2.2. Catalytic activity tests

Typically, the catalytic performances of Ag catalyst were carried out in a fixed-bed flow reactor system, consisting of a quartz reactor tube. The catalysts were held in place between plugs of quartz wool and a K-type thermocouple was placed in the centre of the catalyst bed. Each of the gases in the feed system was controlled individually by mass flow controllers, while *n*-octane and water vapour were separately introduced to the system by means of saturators using Ar as the carrier gas. The *n*-octane saturator was placed in an ice/water bath, where its temperature was carefully controlled while the temperature of $H_2O$ saturator was controlled using a thermostatic bath. All the lines following the water saturator were heated to prevent condensation.

The feed gas stream consisted of 720 ppm NO; 4340–8680 ppm (as $C_1$) HC, 4.3% $O_2$, 7.2% $H_2O$; 7.2% $CO_2$ and Ar balance was introduced to the reactor heated from 150 to 600 °C stepwise at 50 °C intervals remaining at each temperature for 40 min in order to obtain steady state conditions. Note that when using a mixture of hydrocarbons, the concentration of each hydrocarbon used is presented as $C_1$, for example *n*-octane/methanol with 4340/4340 mixture, for which the first number represents the concentration of either *n*-octane or toluene and the second one represents the concentration of methanol. The total gas flow rate was 276 $cm^3\,min^{-1}$ over 276 mg of catalyst which was sieved to obtain particle size of 250–450 μm. The inlet and outlet $NO_x$ concentrations were determined by a Signal 4000VM series chemiluminescence detector. The oxidation of hydrocarbon was measured online using a Bruker Tensor 27 IR spectrometer, fitted with a gas cell of volume 190 $cm^3$.

### 2.3. Fast-transient experiments

Fast switching experiments were performed using a custom-made plug flow reactor which consisted of a quartz tube (3 mm i.d.) enclosed in an electric furnace. The inner diameter was modified in order to reduce the dead volume [27]. A 2.0% $Ag/Al_2O_3$ catalyst sample (100 mg, particle size 250–425 μm) was held in place between two plugs of quartz wool and a thermocouple was placed in the middle of the catalyst bed. The feed gas was composed of 720 ppm NO; 4340 ppm (as $C_1$) *n*-$C_8H_{18}$; 4.3% $O_2$; 7.2% $CO_2$; 7.2% $H_2O$; 4340 ppm (as $C_1$) $CH_3OH$ (when added) and Ar balance. The total flow rate was 200 $cm^3\,min^{-1}$. A fast switching experimental system was applied using helium actuated high speed switching VICI valves. The 4-way valves allowed rapid switching between two gas mixtures in less than 20 ms [24]. Gas flows were carefully equilibrated using micrometric needle valves to adjust the pressure between the gas flows on each side of the four-way valve with a high-sensitivity differential pressure detector. This avoided the production of spikes in the MS signal when switching from one mixture to another. The analysis was carried out with a Hiden Analytical HPR 20 mass spectrometer.

Due to several fragments derived from methanol, three different gas mixtures were used to avoid the overlap of masses. The conversions of $NO_x$, *n*-$C_8H_{18}$ and $CH_3OH$ were obtained using a $^{14}NO$–$C_8H_{18}$–$CH_3OH$ system while $^{15}N_2$ formation was monitored using $^{15}NO$–$C_8H_{18}$–$CH_3OH$ mix. Moreover, $^{15}NO$–$C_8H_{18}$–$CD_3OD$ mixture was used to monitor $D_2$ and $^{15}ND_3$. Kr was added to the methanol containing feed in order to provide an inert internal tracer with which to track the reactant switches. The switching

of methanol in and out of the *n*-octane-SCR reaction over the 2 wt% Ag/Al$_2$O$_3$ catalyst was performed every 60 s for at least 20 cycles at 250, 300 and 350 °C. Quantification of $^{15}N_2$, $^{15}N_2O$, $^{15}ND_3$, and $D_2$ was carried out using 1% N$_2$/He, 2000 ppm N$_2$O/He, 1% NH$_3$/Ar and 5% H$_2$/Ar cylinders, respectively. The calculation of these gases was performed with reference to the Kr signal and subtraction of the blank reactor profile. For the majority of experiments, the following fragmented mass-to-charge (*m/e*) ratios were monitored as a function of time: 2 (H$_2$), 4 (D$_2$), 28 ($^{14}N_2$, CO, CO$_2$), 29 (CH$_3$OH), 30 ($^{14}NO$, $^{15}N_2$, CD$_3$OD), 31 ($^{15}NO$, CH$_3$OH), 32 (O$_2$, CH$_3$OH), 44 (CO$_2$), 46 ($^{14}NO_2$, $^{15}N_2O$), 47 ($^{15}NO_2$), 57 (*n*-C$_8$H$_{18}$) and 82 (Kr).

### 2.4. DRIFTS analysis

*In situ* DRIFTS measurements were performed with a Bruker Vertex 70 FTIR spectrometer equipped with a liquid N$_2$-cooled detector. In a typical experiment, 25 mg of 2.0% Ag/Al$_2$O$_3$ catalyst was placed in a ceramic crucible in the DRIFTS cell.

Prior to the experiments, the catalyst was pre-treated by heating in 5% O$_2$/Ar with a total flow rate of 50 cm$^3$ min$^{-1}$ up to 300 °C for 1 h and then cooled down in flowing Ar to 250 °C. The IR spectrum of the Ag/Al$_2$O$_3$ catalyst at 250 °C under flowing Ar was taken as the background. The 4-way VICI valve was installed to allow us to switch between two gas mixtures. Kr was used a tracer for the switching experiments. The concentrations of the reactants used were 720 ppm NO; 4340 ppm (as C$_1$) *n*-C$_8$H$_{18}$; 4.3% O$_2$; 4.0% H$_2$O; 4340 ppm (as C$_1$) CH$_3$OH (when added), 0.1% Kr (when added); and Ar balance. The total flow rate was 50 cm$^3$ min$^{-1}$.

To investigate the role of methanol on promoting the *n*-octane-SCR reaction over Ag/Al$_2$O$_3$ catalysts, the catalyst was exposed to the *n*-octane-SCR gas feed for 60 min at 250 °C before performing the transient switches of methanol in and out of the *n*-octane-SCR gas mixture every 5 min. The *in situ* DRIFTS spectra were recorded with a resolution of 4 cm$^{-1}$ and with an accumulation of 16 scans every 10 s during transient switches. The DRIFTS spectra were analyzed by the OPUS software.

## 3. Results

### 3.1. Catalytic activity

Fig. 1 shows NO$_x$, *n*-octane, toluene and methanol conversions obtained from NO$_x$ reduction reaction using the individual and combination of the hydrocarbons over a Ag/Al$_2$O$_3$ catalyst. It is seen in Fig. 1a that there is a remarkable improvement of NO$_x$ conversions with both *n*-octane and toluene in the presence of methanol. In the presence of pure *n*-octane, the SCR activity starts at ~250 °C and reaches a broad maximum of >93% NO$_x$ conversion ~400 °C before decreasing to 43% at 550 °C. A similar profile of NO$_x$ conversion with toluene was observed with the profile shifted to higher temperatures. The SCR activity with toluene starts just below 400 °C before reaching a maximum NO$_x$ conversion of 83% at ~500 °C and then decreases to 52% at ~590 °C. However, on addition of methanol into the *n*-octane or toluene-SCR feeds the catalytic reduction was of NO$_x$ began just above 150 and 200 °C before reaching the maximum NO$_x$ conversions (>93%) at 250 and 270 °C for the *n*-octane/methanol and toluene/methanol systems, respectively. In addition, the light-off temperature at which 50% hydrocarbon conversion was obtained was shifted from 380 to 290 °C and from 450 °C to 310 °C for the pure *n*-octane and toluene to *n*-octane/methanol and toluene/methanol mixtures, respectively, as shown in Fig. 1b.

To examine if the increased activity was simply due to the use of more hydrocarbon reductant in the mixture, the activity tests were
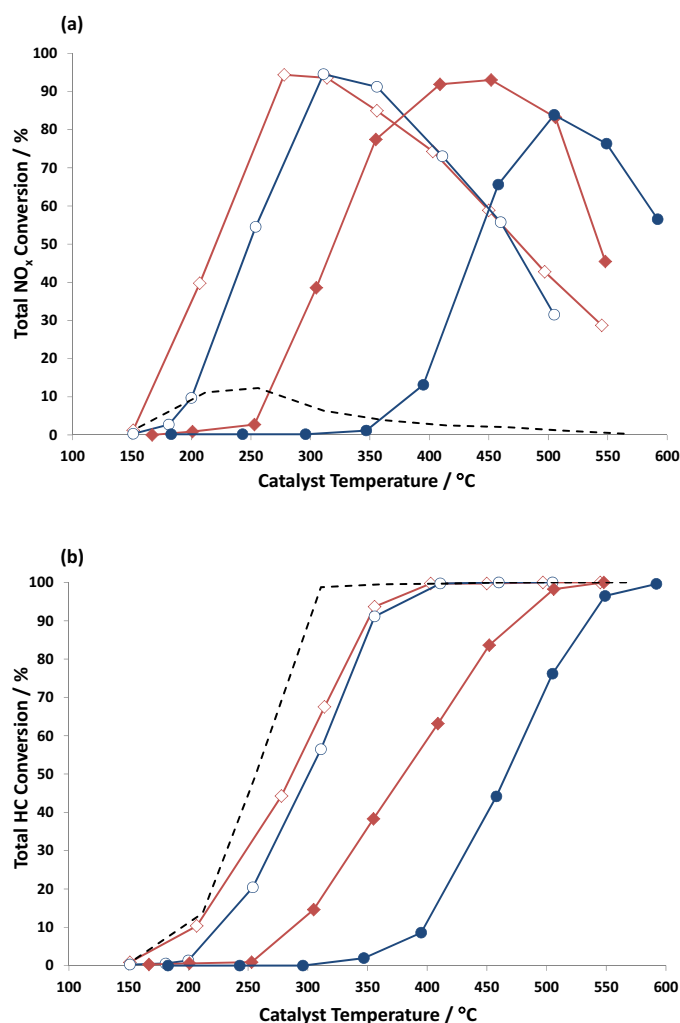


**Fig. 1.** NO$_x$ (a) and hydrocarbon (b) conversions as a function of catalyst temperature during the HC-SCR of NO$_x$ reaction over 2 wt% Ag/Al$_2$O$_3$: with octane/methanol (◇) and toluene/methanol (○) mixtures in comparison with octane (◆), toluene (●) and methanol (—). Feed composition: 720 ppm NO, 4340 ppm (as C$_1$) *n*-C$_8$H$_{18}$ and C$_7$H$_8$, 4340 ppm CH$_3$OH (when added), 4.3% O$_2$, 7.2% CO$_2$, 7.2% H$_2$O and Ar balance. The total flow rate and space velocity was 276 cm$^3$ min$^{-1}$ and 60,000 cm$^3$ g$^{-1}$ h$^{-1}$, respectively.

performed by fixing the C$_1$/NO ratio at 6 and the results are shown in Fig. 2.

Although the SCR of NO$_x$ reaction with methanol alone showed a low-temperature activity over Ag/Al$_2$O$_3$ catalyst, the maximum NO$_x$ conversion was very poor and it was found to be *ca.* 13% at 250 °C. However, Fig. 2 shows that there is a trend of improved NO$_x$ conversion when lowering the concentration of either *n*-octane or toluene but increasing the concentration of methanol even though the C$_1$/NO ratio remains constant. The low temperature SCR activity was enhanced below 350 °C. However, this depends on the concentration of methanol present in the SCR feed. For example, in the case of *n*-octane/methanol or toluene/methanol for both 3840/500 and 3340/1000 mixtures, although NO$_x$ conversion at below 250 °C is lower than that obtained from the SCR with pure methanol, NO$_x$ conversion is slightly improved at temperatures between 250 and 350 °C. Fig. 2 also shows that the optimal deNO$_x$ performance can be achieved when using either *n*-octane/methanol or toluene/methanol with a ratio of 2340/2000 ppm with respect to the reasonable light off temperature of NO$_x$ reduction and operational temperature window. It is interesting to see that the conversion of NO$_x$ is also improved below 300 °C when further
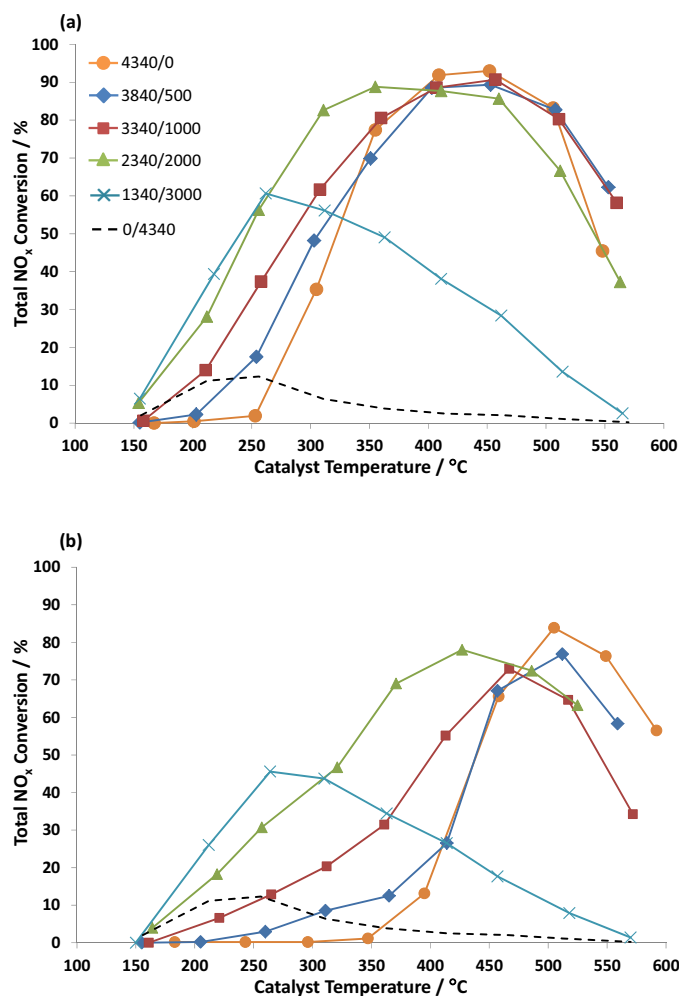
**Fig. 2.** $NO_x$ conversions as a function of temperature during the HC-SCR of $NO_x$ reaction over 2 wt% $Ag/Al_2O_3$ with octane/methanol (a) and toluene/methanol (b) mixtures: 4340/0 ppm (●), 3840/500 ppm (♦), 3340/1000 ppm (■), 2340/2000 ppm (▲), 1340/3000 ppm (×). Feed composition: 720 ppm NO, 4340 ppm (as $C_1$) HC, 4.3% $O_2$, 7.2% $CO_2$, 7.2% $H_2O$ and Ar balance. The total flow rate and space velocity was 276 cm³ min⁻¹ and 60,000 cm³ g⁻¹ h⁻¹, respectively.

lowering the concentration of *n*-octane or toluene to 1340 ppm and increasing the concentration of methanol to 3000 ppm. The catalytic activity of $NO_x$ reduction increases to the maximum value at about 260 °C, giving the $NO_x$ conversion of 61% and 46% for *n*-octane/methanol and toluene/methanol systems, respectively. However, the SCR activity under these conditions significantly decreases at temperatures above 300 °C due to complete oxidation of methanol and hydrocarbons.

### 3.2. Fast-switching and gas phase analysis

The fast-transient experiments were performed using three different combinations of reactants in order to observe the gas phase reactants and products and to avoid the difficulty derived from overlapping masses. The calculated results from these experiments are summarized in Table 1.

### 3.2.1. $^{14}NO–C_8H_{18}–CH_3OH$

Fig. 3 shows the fast-transient responses in $NO_x$ and *n*-octane conversions as well as the outlet methanol concentration during the switching of methanol into and out of the *n*-octane-SCR feed as a function of catalyst bed temperature. The overall trends for the conversions of $NO_x$ and *n*-octane can be seen from Fig. 3a and b,
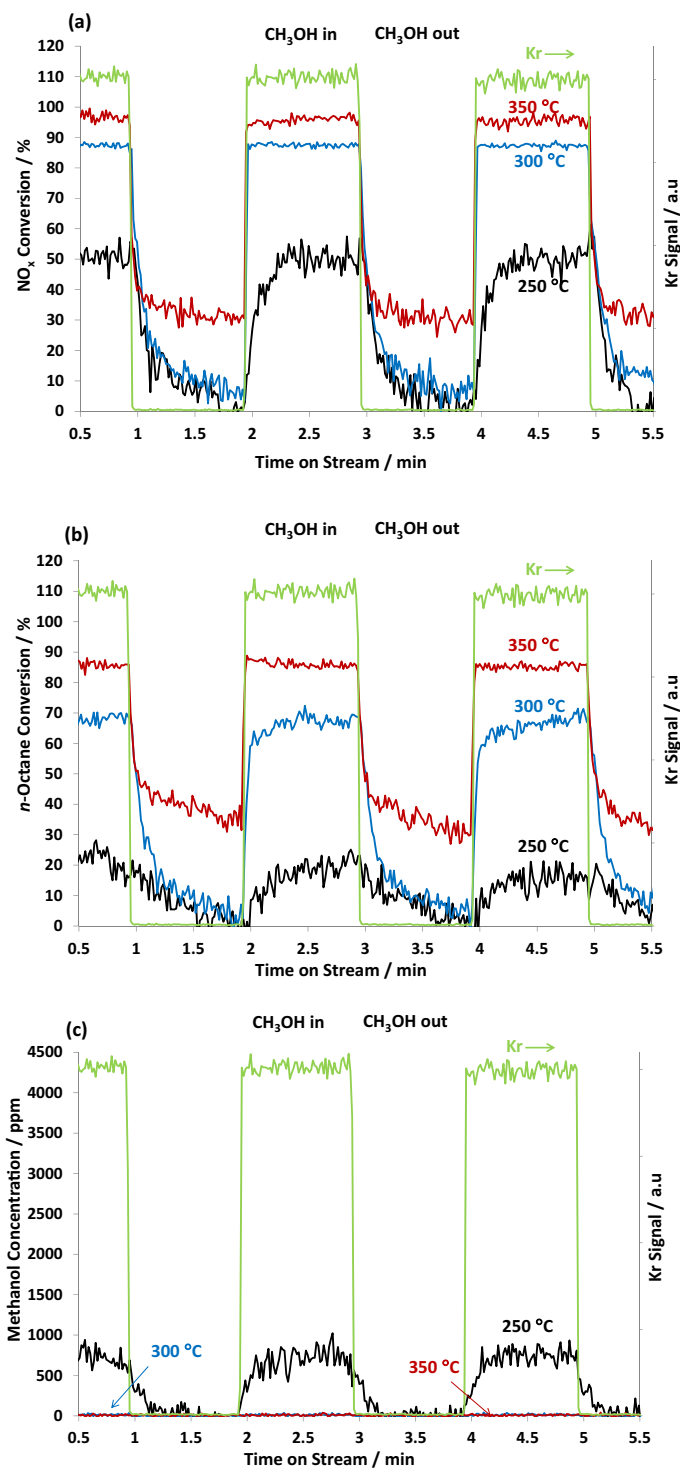






**Fig. 3.** Changes in $^{14}NO_x$ (a), octane (b) conversions and methanol (c) concentration over time as a function of catalyst temperature during 60 s switches of methanol in and out of the octane-SCR of $NO_x$ reaction over 2 wt% $Ag/Al_2O_3$. Feed composition: 720 ppm NO, 4340 ppm (as $C_1$) *n*-$C_8H_{18}$, 4340 ppm $CH_3OH$ (when added) 4.3% $O_2$, 7.2% $CO_2$, 7.2% $H_2O$, 1% Kr (when added) and Ar balance. The total flow rate and space velocity was 200 cm³ min⁻¹ and 120,000 cm³ g⁻¹ h⁻¹, respectively.

respectively. As the reaction temperature increased, the SCR activity with *n*-octane over the Ag catalysts increased.

In the present study, upon introduction of methanol at 250 °C, the conversion of both $NO_x$ and *n*-octane slowly increases with a small time lag of <20 s compared with the tracer before reaching steady-state values of about 53% and 22%, respectively. Methanol is

**Table 1**
[a]Conversions of reactants and formations of products during a fast-transient switching under the SCR reaction conditions with and without adding methanol as a function of catalyst temperature.

| | Feed | Temperature (°C) | | |
| --- | --- | --- | --- | --- |
| | | 250 | 300 | 350 |
| $NO_x$ conversion[b] (%) | With $CH_3OH$ | 53 | 87 | 98 |
| | Without $CH_3OH$ | 2 | 5 | 30 |
| $C_8H_{18}$ conversion[b] (%) | With $CH_3OH$ | 22 | 68 | 86 |
| | Without $CH_3OH$ | 1 | 5 | 36 |
| $CH_3OH$ conversion[b] (%) | With $CH_3OH$ | 83 | 100 | 100 |
| | Without $CH_3OH$ | – | – | – |
| $^{15}N_2$ production[c,d] (ppm) | With $CH_3OH$ | 172 (90) | 290 (92) | 352 (99.8) |
| | Without $CH_3OH$ | Trace | Trace | 105 (97.2) |
| $D_2$ formation[e] (ppm) | With $CD_3OD$ | 34 | 12 | 0 |
| | Without $CD_3OD$ | 0 | 0 | 0 |
| $^{15}ND_3$ formation[e] (ppm) | With $CD_3OD$ | 5 | 11 | 0 |
| | Without $CD_3OD$ | 0 | 0 | 0 |

<sup>a</sup> All the calculated values are averaged from five different cycles during transient switches of methanol in and out of the octane-SCR feed.
<sup>b</sup> Calculated using $^{14}NO–C_8H_{18}–CH_3OH$ system.
<sup>c</sup> Calculated using $^{15}NO–C_8H_{18}–CH_3OH$ system.
<sup>d</sup> The numbers in parenthesis represent the selectivity of $N_2$ production.
<sup>e</sup> Calculated using $^{15}NO–C_8H_{18}–CD_3OD$ system.

not completely converted at 250 °C (Fig. 3c) and this suggests that the methanol-SCR reaction also contributes to the $NO_x$ conversion at this temperature. On adding methanol, an instantaneous increase in both $NO_x$ and octane conversions was observed at 300 and 350 °C, giving an average $NO_x$ conversion of 87% and 98%, respectively, and an average $n$-octane conversion of 68% and 86%, respectively (Table 1). Similar features can be seen at all three temperatures after methanol was removed from the gas feed. The $NO_x$ conversion decreased gradually with the time lag of ~30 s compared with the tracer to 0%, 5% and 30% at 250 °C, 300 °C and 350 °C, respectively. It should be noted that at above 250 °C complete conversion of methanol was observed.

In this set of experiments, we observed changes in the MS signal of $m/e = 2$, which may be related to hydrogen formation during the switches of methanol into and out of the $n$-octane-SCR reaction at 250, 300 and 350 °C. These results are further described and discussed in Section 3.2.3.

### 3.2.2. $^{15}NO–C_8H_{18}–CH_3OH$

Fig. 4 shows the effect of methanol on the evolution of gas phase $^{15}N_2$ production, monitored during the transient switching. The changes in $^{15}N_2$ production showed similar trends for
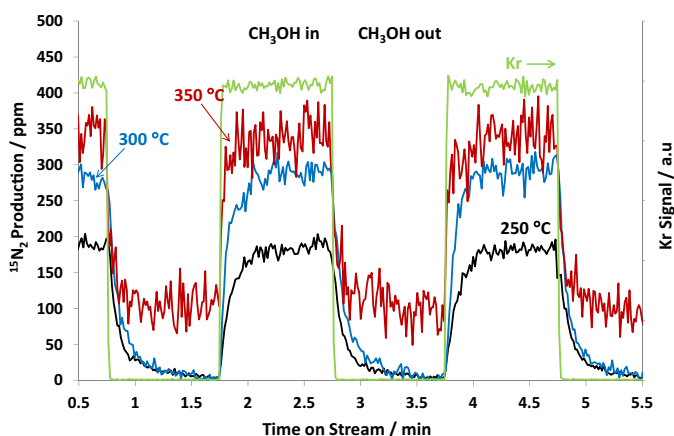


**Fig. 4.** Changes in $^{15}N_2$ formation over time as a function of catalyst temperature during 60 s switches of methanol in and out of the octane-SCR of $NO_x$ reaction over 2 wt% $Ag/Al_2O_3$. Feed composition: 720 ppm $^{15}NO$, 4340 ppm (as $C_1$) $n$-$C_8H_{18}$, 4340 ppm $CH_3OH$ (when added) 4.3% $O_2$, 7.2% $CO_2$, 7.2% $H_2O$, 1% Kr (when added) and Ar balance. The total flow rate and space velocity was 200 cm³ min⁻¹ and 120,000 cm³ g⁻¹ h⁻¹, respectively.

each temperature and were found to increase with temperature. As found with the $NO_x$ conversion profile (Fig. 3a) at 250 °C, the evolution of $^{15}N_2$ increased slowly to its maximum concentration of ~172 ppm upon introduction of methanol and then gradually decreased to 0 ppm upon the removal of the methanol over the course of 1 min. At 300 °C, it is also seen that the production of $^{15}N_2$ increased slowly to ~290 ppm when methanol was present in the gas feed. After removing methanol from the feed, there is a slow decrease in $^{15}N_2$ production over the course of 1 min, as seen at 250 °C. The similar profile of $N_2$ behaviour was also observed at 350 °C. At 350 °C, the addition of methanol resulted in an initial sharp increase in $^{15}N_2$ production, reaching a concentration of ~352 ppm before rapidly decreasing to ~100 ppm after removing methanol from the feed. With a remarkable improvement of $NO_x$ conversion by adding methanol, the $N_2$ selectivity, summarized in Table 1, increased with increasing temperature to 90, 92 and 99% at 250, 300 and 350 °C, respectively. For a comparison, the result obtained at 200 °C (see Figs. S1 and S2) showed lower selectivity of $^{15}N_2$ (~63%) with increased $^{15}N_2O$ formation (~31%). The trend of the selectivity of $N_2$ in this study was similar to that found for the SCR activity with $n$-octane on its own whether with or without $H_2$ [27,62].

### 3.2.3. $^{15}NO–C_8H_{18}–CD_3OD$

As discussed in Section 3.2.1 the MS signal associated with hydrogen ($m/e = 2$) was detected during the switching $CH_3OH$ into and out of the SCR feed at 250 and 300 °C. In order to clarify the effect of methanol, further experiments were carried out by using both isotopically labelled $^{15}NO$ and deuterated $CD_3OD$ as reactants in order to see whether or not $D_2$ can be formed from methanol. Fig. 5 shows the transient responses in the formation of $D_2$ and $^{15}ND_3$ during the switching of $CD_3OD$ into and out of the $n$-octane-SCR feed as a function of reaction temperature. Importantly, from Fig. 5a it is clear that there is a release of $D_2$ observed at both 250 and 300 °C of ~35 and ~12 ppm. There was no observed release of $D_2$ at 350 °C presumably due to its complete combustion at the higher temperature. Upon removal of methanol from the $n$-octane-SCR feed, a slow decrease in $D_2$ concentration was seen, suggesting that some surface species derived from partial oxidation of methanol may be responsible for deuterium formation.

In addition to $D_2$ formation, there are changes in the MS signal at $m/e = 21$ and this is proposed to be $^{15}ND_3$. Fig. 5b shows that, when deuterated methanol was present in the feed at 250 and 300 °C, ca. 5 and 10 ppm $^{15}ND_3$ was observed, respectively. Again, at 350 °C,
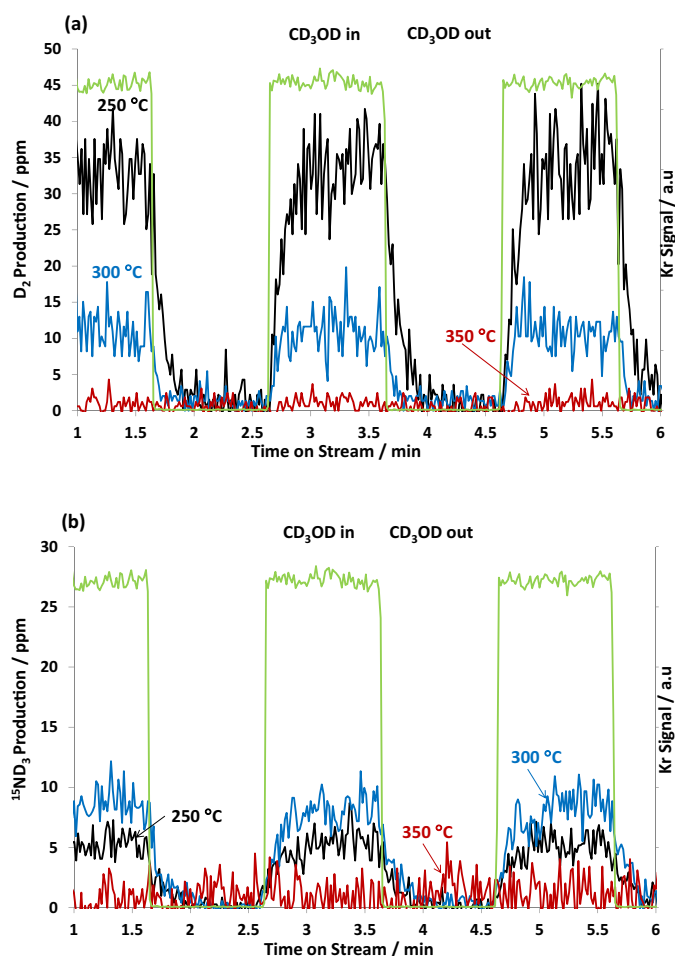
**Fig. 5.** Changes in $D_2$ (a) and $^{15}ND_3$ (b) formation over time as a function of catalyst temperature during 60 s switches of deuterated methanol in and out of the octane-SCR of $NO_x$ reaction over 2 wt% $Ag/Al_2O_3$. Feed composition: 720 ppm $^{15}NO$, 4340 ppm (as $C_1$) $n$-$C_8H_{18}$, 4340 ppm $CD_3OD$ (when added) 4.3% $O_2$, 7.2% $CO_2$, 7.2% $H_2O$, 1% Kr (when added) and Ar balance. The total flow rate and space velocity was 200 $cm^3$ $min^{-1}$ and 120,000 $cm^3$ $g^{-1}$ $h^{-1}$, respectively.

there was no release of gas phase $^{15}ND_3$ formation, probably due to its complete consumption to form $^{15}N_2$.

### 3.3. In situ DRIFTS analysis

*In situ* DRIFTS analysis was performed in order to identify surface species present during the methanol enhanced SCR reaction. Please note that, in this study, we do not aim to identify which surface species are involved in hydrogen production but rather to investigate the nature of some surface species that are responsible for the $N_2$ production. Fig. 6 shows the typical *in situ* DRIFTS spectra obtained under 60 min steady state conditions during the reaction at 300 °C in the presence and absence of methanol. The spectra observed under steady state conditions with and without adding methanol show significant changes in the bands which are similar to those found using $n$-octane and $n$-decane as reductants in the presence and absence of $H_2$ [8,24–26,62,63].

The bands between 2880 and 3000 $cm^{-1}$ can be attributed predominantly to $-CH_3$ and $-CH_2-$ stretching vibrations of gas phase and adsorbed hydrocarbons and partially oxidized hydrocarbon species [3,8,12,13,25,26,63–66]. The bands appearing between 1200 and 1800 $cm^{-1}$ are due to a large number of adsorbed species including nitrates (1308, 1545 $cm^{-1}$), carboxylates (1595 $cm^{-1}$), acetates (1464 $cm^{-1}$) and formates (1377,
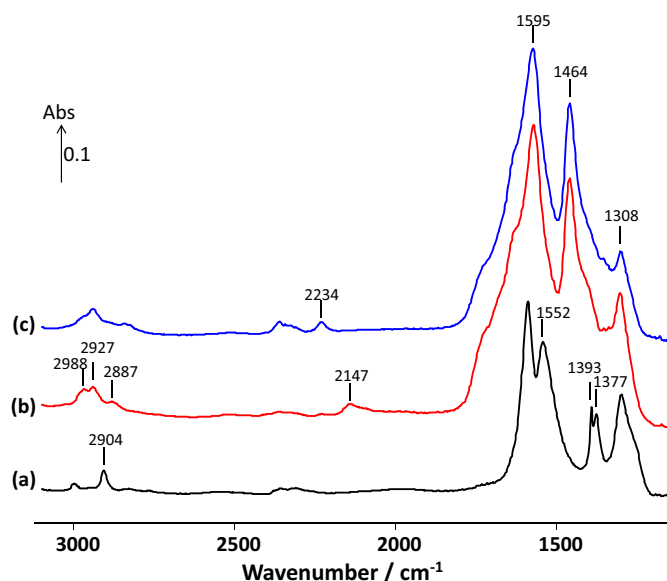


**Fig. 6.** A comparison of *in-situ* DRIFTS spectra obtained after 60 min under steady state conditions during the SCR reaction with methanol (a), octane (b) and methanol + octane (c) at 300 °C. Feed composition: 720 ppm NO, 4340 ppm (as $C_1$) HC, 4.3% $O_2$, 4.0% $H_2O$ and Ar balance.

1393 $cm^{-1}$) [3,8,12,13,25,26,63–66]. The IR bands observed at 2234 and 2147 $cm^{-1}$ can be assigned to isocyanates ($-NCO$) absorbed on alumina [8,25,26,63–66] and cyanide ($-CN$) species absorbed on Ag sites [8,24–26,63–66], respectively.

There has been a significant amount of debate concerning the role of $-NCO$ and $-CN$ surface species in connection with the SCR reaction mechanism [5–8,8,25–33,51–53,62–66]. In particular, the involvement of $-NCO$ species in the final step to form gas phase $N_2$ has been examined in detail and there is general agreement that this is important in the overall mechanism [8,25–27,62–66]. Therefore, we will focus on the surface species in the region between 2000 and 2300 $cm^{-1}$ in this study. It is clearly seen in Fig. 6 that there are noticeable differences in the DRIFTS spectra recorded under the SCR reaction conditions at 300 °C. In the case of the SCR with pure methanol (Fig. 6a), the surface species are mainly associated with nitrates, carboxylates and formates and $-NCO$ and $-CN$ surface species are not observed. In Fig. 6b the SCR with pure $n$-octane shows mostly cyanides at 2147 $cm^{-1}$ and there is very little formation of $-NCO$ after 60 min under reaction conditions. Interestingly, the $-NCO$ peak at 2234 $cm^{-1}$ is observed when co-feeding methanol in the $n$-octane-SCR feed with a concomitant reduction in the $-CN$ species observed (Fig. 6c).

In order to probe the relevance of differences in surface species observed in Fig. 6, *in situ* DRIFTS spectra were collected at 10 s intervals during a series of cycles switching methanol into and out of the octane-SCR feed. In this experiment, the catalyst was first exposed to the $n$-octane-SCR feed at 300 °C for 60 min to allow the cyanides to be formed on the catalyst surface. Thereafter, methanol was switched into and out of the $n$-octane-SCR feed every 5 min. The changes in both $-NCO$ and $-CN$ surface species during 5 min switches in the first cycle are presented in Fig. 7. It is evident from Fig. 7a that the intensity of the adsorbed $-CN$ band at 2147 $cm^{-1}$ starts to decrease when switching methanol into the $n$-octane-SCR feed. At the same time, there is an increase in the intensity of adsorbed $-NCO$ species. This suggests that the addition of methanol to the $n$-octane-SCR mixture removes the cyanides, perhaps on Ag sites [24–26,63–66], or converts the cyanides to NCO species as reported in the literature [63–66]. In contrast, upon removal of methanol from the $n$-octane-SCR feed the intensity of cyanides
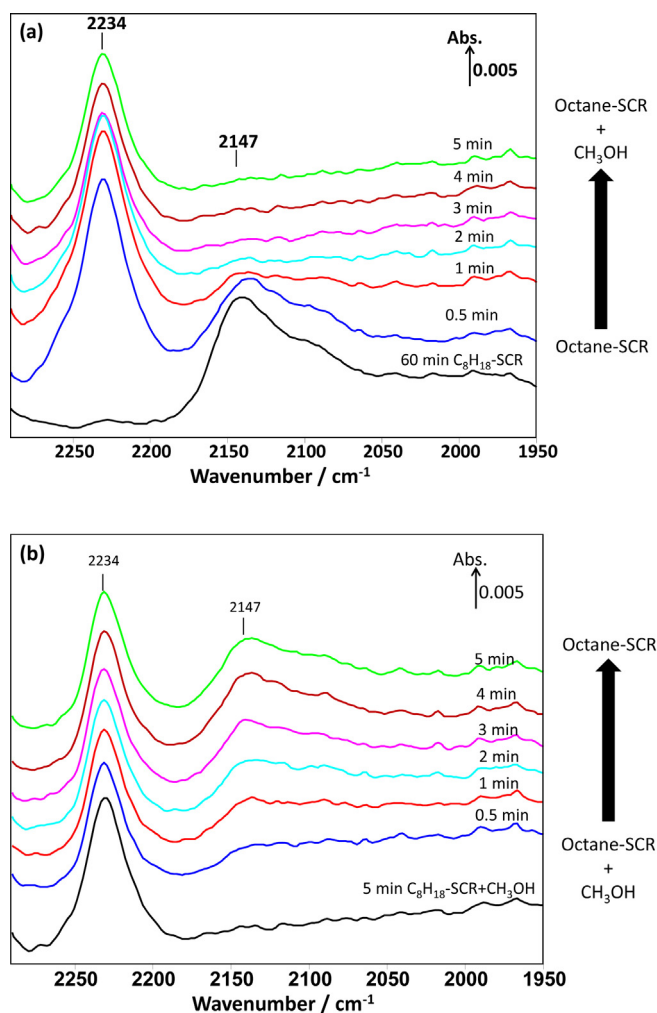
**Fig. 7.** Changes in intensity of *in situ* DRIFTS spectra obtained during 5 min switching methanol in (a) and out (b) of the octane-SCR feed at 300 °C. Note that the catalyst was exposed to the full octane-SCR gas mix in the absence of methanol for 60 min before cycling methanol in and out of the SCR mix.

increases over the course of 5 min; however, there is little decrease in the —NCO band.

## 4. Discussion

The results obtained from the catalytic activity tests under steady state reaction conditions (see Figs. 1 and 2) showed for the first time a significant improvement of the SCR activity by using a mixture of either *n*-octane/methanol or toluene/methanol mixtures as reducing agents. As reported in the literature [41,49,50], the SCR activity with pure methanol is very poor. However, in this study, the promoting effect of methanol on the SCR activity has been discovered by the use of combinations of methanol and *n*-octane or toluene. Whilst there is still *n*-octane and toluene present at the higher temperatures when mixed with the methanol, as the $C_1$/NO ratio is kept constant in the experiments, the concentration of the reductant is lower once all the methanol has been reacted compared with the pure hydrocarbon and resulting in a decrease in $NO_x$ conversion profile at high temperatures.

Figs. 3–5 showed the transient response of gas phase reactants and products during the switches of methanol into and out of the *n*-octane-SCR feed. The addition of methanol enhances the conversions of $NO_x$ (Fig. 3a) and *n*-octane (Fig. 3b) and the production of $N_2$ (Fig. 4). This phenomenon is similar to the $H_2$ effect reported

previously [27]. In addition, release of hydrogen and ammonia was detected during the transient experiments at 250 and 300 °C (Fig. 5).

The key features observed from these fast-transient experiments are associated with the time lags in the response of reactants and products when removing methanol from the *n*-octane-SCR gas feed. Fig. 3a and b shows that both $NO_x$ and *n*-octane conversions slowly decreased over the course of 1 min with a time lag of ∼35 s. This means that methanol has a residual effect on the $NO_x$ conversion upon removal of methanol from the SCR feed. When considering the outlet concentration of methanol during the transient switches it was found in Fig. 3c that at 250 °C the outlet concentration of methanol was ∼800 ppm equating to ∼81% conversion and this then slowly decreased to 0 ppm within 15 s when methanol was switched out. Therefore, it is possible that some remaining gas phase methanol may be responsible for the gradual decrease in both $NO_x$ and *n*-octane conversions after removing methanol from the feed at 250 °C. However, blank switches without the catalyst in the reactor were performed and showed that the concentration of methanol decreased from 4340 to *ca.* 10 ppm within 2 s of the switch. Likewise the time lag (35 s) for $NO_x$ and octane conversions is much longer than that found for the methanol in a blank experiment. However, we cannot exclude the possibility that methanol is adsorbed and then slowly desorbed from the catalyst support at the low temperature used in this experiment. The same profiles of $^{15}N_2$ production upon removal of methanol from the octane-SCR feed were observed as shown in Fig. 4. One possible explanation is that the addition of methanol may result in the storage of surface species derived from added methanol, which can then be used for the SCR reaction after removing methanol from the feed.

The *in situ* DRIFTS measurements were carried out to investigate the surface species that may be involved in this promotional effect of methanol. With methanol on its own (Fig. 6a) surface showed mainly formates and nitrate species. In contrast, the DRIFTS spectra with pure *n*-octane and an *n*-octane/methanol mixture showed a wide range of species present, most importantly, isocyanate species were present when co-feeding methanol in the octane-SCR reaction. There is a general agreement in the literature [5–8,8,25–27,51–53,62–66] that isocyanates are key intermediates and involved in the SCR reaction mechanism to form $N_2$. It is evident in Fig. 7 that there are changes in intensity of cyanide and isocyanate bands during the switches of methanol in and out of the *n*-octane-SCR feed.

To clarify the behaviour of both —NCO and —CN species, the dynamic changes in the integrated peak areas of —NCO and —CN are presented in Fig. 8. It should be noted that the changes of —NCO and —CN species are NOT straightforwardly comparable with the results obtained from the fast transient experiments due to the dead volume of the DRIFTS cell. However, the semi-quantitative results do provide some insights into how methanol may be involved in the reaction mechanism. It is clearly seen in Fig. 8a that the addition of methanol to the *n*-octane-SCR feed results in a decrease in the concentration of —CN species over the course of 5 min with 90% removal after 1 min. In addition, there was a rapid increase in concentration of —NCO species up to 1 min which, thereafter, reduced in intensity slowly to ∼70% of the peak maximum after 3.5 min and then levelling off at this value. These results are similar to the promotional effect of hydrogen on the HC-SCR reaction previously reported [25]. In these studies, the role of hydrogen is thought to be to remove a poison that inhibits the SCR reaction. Burch et al. [24] and Sazama et al. [63] have proposed that one of the key roles of $H_2$ is to eliminate $Ag^+CN$ species, which blocks the active sites during the SCR reaction. This is consistent with the methanol results which show a significant drop in —CN, as can be seen in Fig. 6b, —CN species are dominant in the case of *n*-octane-SCR reaction. Bion et al. [65] suggested that the slow step in the SCR reaction is the
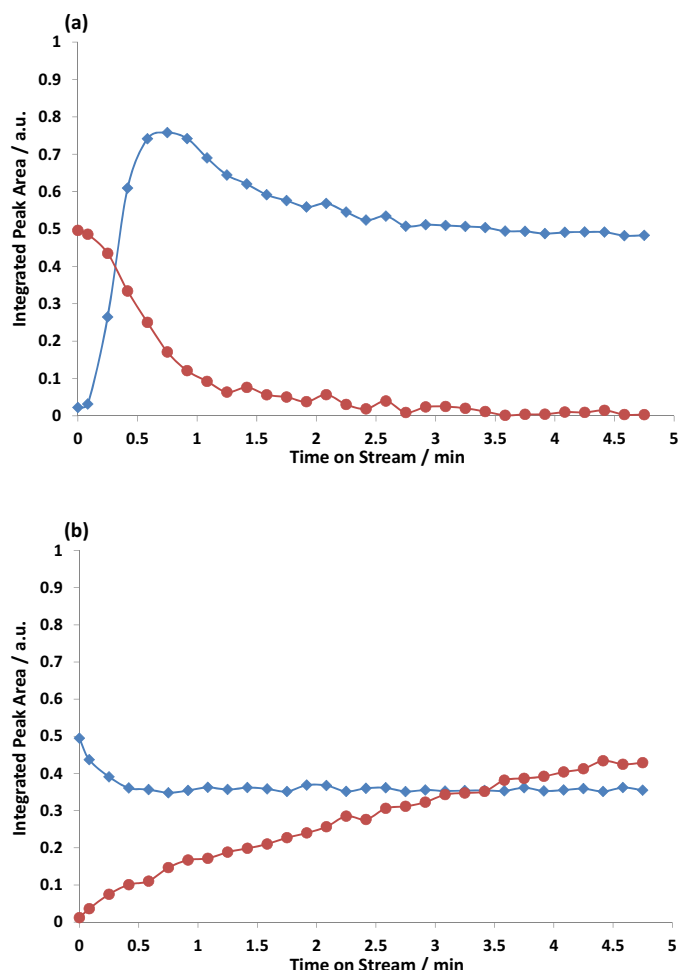
**Fig. 8.** Dynamic changes in integrated peak areas of both —NCO (♦) and —CN (●) species obtained from *in situ* DRIFTS spectra corresponding to Fig. 7 during 5 min switching methanol in (a) and out (b) of the octane-SCR feed at 300 °C. Note that the catalyst was exposed to the full octane-SCR gas mix in the absence of methanol for 60 min before cycling methanol into and out of the SCR mix. The first point for all cases represents the value calculated just before switching from one feed to another.

transformation of $Ag^+CN$ species to $Al^{3+}NCO$ species. Therefore, it is sensible to propose that one role of $H_2$ could be to accelerate this slow step in the SCR reaction. Chansai and co-workers [25,26] also reported the use of the short time on stream (STOS) technique to investigate the effect of hydrogen on the *n*-octane-SCR reaction and concluded that only a fraction of —NCO species, adsorbed very close to Ag active sites, is very reactive and involved in the SCR reaction. Therefore, it is possible to conclude that the promoting effect of methanol could occur *via* the effect of $H_2$, as shown by the release of $H_2/D_2$ in Fig. 5a. The origin of the hydrogen is not clear although it is clear from the isotope studies that it comes from methanol, possibly *via* the OH (OD) group since this hydrogen (deuterium is easily removed from methanol when it adsorbs.

It is also shown in Fig. 8b that when removing methanol from the feed the —CN band starts to increase as the reactive —NCO species start to decrease due to the fact that stored —NCO species can be converted by NO or by $NO + O_2$ to gas phase $N_2$ as reported previously [62–66]. This may explain the reason why there was a slow decrease in $NO_x$ conversion and $N_2$ production on switching methanol out of the SCR feed (see Fig. 4). It is interesting to note that —NCO species are not completely removed due to unreactive —NCO species stored on the $Al_2O_3$ support. This similar observation has been reported by Chansai et al. [25,26], who applied the short time

on stream (STOS) technique to investigate the role of —NCO species and the effect of $H_2$ on the SCR activity over $Ag/Al_2O_3$ catalyst.

The DRIFTS results can also explain the release of $NH_3$ during methanol switches (see Fig. 5b). Breen et al. [27] extensively investigated the effect of $H_2$ on the *n*-octane-SCR reaction over $Ag/Al_2O_3$ catalyst using a fast-transient technique to probe the role of $H_2$ and the behaviours of gas phase reactants and products. It was observed that ammonia was formed and detected when switching $H_2$ into the octane-SCR feed. In this case, the $NH_3$ formation may be associated with the hydrolysis of the —NCO species formed on adding methanol into the SCR feed [27,62–66]. This $NH_3$ can then interact with $NO + O_2$ as an additional route to form $N_2$ [27,62–66].

As presented and discussed above, it is seen that the catalytic reduction of $NO_x$ with methanol alone is very poor throughout a wide range of temperatures. However, together with either *n*-octane or toluene, methanol in the SCR feed has been found to have a remarkable effect on the overall DeNO$_x$ performance in which the profiles of $NO_x$ conversion are shifted to low temperatures below 350 °C. It is shown that methanol plays an important role in enhancing the SCR activity. Since small amounts of hydrogen and ammonia were detected together with an improved $NO_x$ conversion, it is possible that the effect of methanol could occur similarly to the $H_2$ effect, perhaps *via* a partial oxidation of $CH_3OH$ to $H_2$ [34–36]. The DRIFTS analysis presented herein also showed the disappearance of the —CN band upon introduction of methanol to the octane-SCR feed, it is also possible to postulate that the methanol reacts or displaces the —CN species and thus removes a potential poison from the silver [49,67]. This has also been suggested as the role of hydrogen in its promotion of the DeNO$_x$ reaction of similar catalyst systems [8,24,27,62,63].

## 5. Conclusions

The addition of methanol to the HC-SCR reaction results in a remarkable improvement in the low temperature activity of a $Ag/Al_2O_3$ catalyst, despite the fact that methanol on its own is not active for the HC-SCR reaction.

The use of a fast transient switching system showed that the addition of methanol enhances the conversions of both $NO_x$ and octane and the production of $N_2$ with high selectivity in comparison with those observed with octane and toluene on their own. This phenomenon is similar to the $H_2$ effect and it is notable that hydrogen and ammonia were detected during the methanol transient experiments.

DRIFTS analysis has revealed that —NCO species are formed when adding methanol into the octane-SCR feed while —CN species are removed/consumed from the surface of the Ag. These —NCO species may play a vital role in promoting the catalytic activity of $NO_x$ reduction but perhaps more importantly the methanol can also remove cyanide species from the silver. Whether this occurs through a methanol-derived species or *via* the formation of hydrogen is not yet clear.

### Appendix A. Supplementary data

Supplementary data associated with this article can be found, in the online version, at http://dx.doi.org/10.1016/j.apcatb.2014.05.040.

# References

[1] K.A. Bethke, H.H. Kung, J. Catal. 172 (1997) 93–102.
[2] R. Burch, J.P. Breen, F.C. Meunier, Appl. Catal., B: Environ. 39 (2002) 283–303.
[3] A. Iglesias-Juez, A.B. Hungría, A. Martínez-Arias, A. Fuerte, M. Fernándezcía, J.A. Anderson, J.C. Conesa, J. Soria, J. Catal. 217 (2003) 310–323.
[4] E.F. Iliopoulou, A.P. Evdou, A.A. Lemonidou, I.A. Vasalos, Appl. Catal., A: Gen. 274 (2004) 179–189.
[5] J. Wang, H. He, Q. Feng, Y. Yu, K. Yoshida, Catal. Today 93–94 (2004) 783–789.
[6] H. He, Y. Yu, Catal. Today 100 (2005) 37–47.
[7] L.-E. Lindfors, K. Eränen, F. Klingstedt, D.Y. Murzin, Top. Catal. 28 (2004) 185–189.
[8] K. Shimizu, A. Satsuma, Phys. Chem. Chem. Phys. 8 (2006) 2677–2695.
[9] V. Demidyak, C. Hardacre, R. Burch, A. Mhadeshwar, D. Norton, D. Hancu, Catal. Today 164 (2011) 515–519.
[10] X. She, M. Flytzani-Stephanopoulos, J. Catal. 237 (2006) 79–93.
[11] K. Takagi, T. Kobayashi, H. Ohkita, T. Mizushima, N. Kakuta, A. Abe, K. Yoshida, Catal. Today 45 (1998) 123–127.
[12] A. Sultana, M. Haneda, T. Fujitani, H. Hamada, Catal. Lett. 114 (2007) 96–102.
[13] J. Li, Y. Zhu, R. Ke, J. Hao, Appl. Catal., B: Environ. 80 (2008) 202–213.
[14] H. Kannisto, H.H. Ingelsten, M. Skoglundh, J. Mol. Catal. A: Chem. 302 (2009) 86–96.
[15] V.I. Pârvulescu, B. Cojocaru, V. Pârvulescu, R. Richards, Z. Li, C. Cadigan, P. Granger, P. Miquel, C. Hardacre, J. Catal. 272 (2010) 92–100.
[16] A. Martínez-Arias, M. Fernández-García, A. Iglesias-Juez, J.A. Anderson, J.C. Conesa, J. Soria, Appl. Catal., B: Environ. 28 (2000) 29–41.
[17] K. Shimizu, A. Satsuma, T. Hattori, Appl. Catal., B: Environ. 25 (2000) 239–247.
[18] K. Shimizu, J. Shibata, H. Yoshida, A. Satsuma, T. Hattori, Appl. Catal., B: Environ. 30 (2001) 151–162.
[19] K. Ralphs, C. D'Agostino, R. Burch, S. Chansai, L.F. Gladden, C. Hardacre, S.L. James, J. Mitchell, S.F.R. Taylor, Catal. Sci. Technol. 4 (2013) 531–539.
[20] V. Houel, D. James, P. Millington, S. Pollington, S. Poulston, R. Rajaram, R. Torbati, J. Catal. 230 (2005) 150–157.
[21] V. Houel, P. Millington, R. Rajaram, A. Tsolakis, Appl. Catal., B: Environ. 73 (2007) 203–207.
[22] V. Houel, P. Millington, R. Rajaram, A. Tsolakis, Appl. Catal., B: Environ. 77 (2007) 29–34.
[23] J.P. Breen, R. Burch, Top. Catal. 39 (2006) 53–58.
[24] R. Burch, J.P. Breen, C.J. Hill, B. Krutzsch, B. Konrad, E. Jobson, L. Cider, K. Eränen, F. Klingstedt, L.E. Lindfors, Top. Catal. 30–31 (2004) 19–25.
[25] S. Chansai, R. Burch, C. Hardacre, J. Breen, F. Meunier, J. Catal. 276 (2010) 49–55.
[26] S. Chansai, R. Burch, C. Hardacre, J. Breen, F. Meunier, J. Catal. 281 (2011) 98–105.
[27] J.P. Breen, R. Burch, C. Hardacre, C.J. Hill, C. Rioche, J. Catal. 246 (2007) 1–9.
[28] S. Satokawa, J. Shibata, K. Shimizu, A. Satsuma, T. Hattori, Appl. Catal., B: Environ. 42 (2003) 179–186.
[29] J. Shibata, Y. Takada, A. Shichi, S. Satokawa, A. Satsuma, T. Hattori, J. Catal. 222 (2004) 368–376.
[30] S. Satokawa, J. Shibata, K. Shimizu, A. Satsuma, T. Hattori, T. Kojima, Chem. Eng. Sci. 62 (2007) 5335–5337.
[31] A. Satsuma, J. Shibata, A. Wada, Y. Shinizaki, T. Hattori, Stud. Surf. Sci. Catal. 145 (2003) 235–238.
[32] J. Shibata, Y. Takada, A. Shichi, S. Satokawa, A. Satsuma, T. Hattori, Appl. Catal., B: Environ. 54 (2004) 137–144.
[33] J. Shibata, K.-I. Shimizu, Y. Takada, A. Shichi, H. Yoshida, S. Satokawa, A. Satsuma, T. Hattori, J. Catal. 227 (2004) 367–374.
[34] L. Mo, A.H. Wan, X. Zheng, C.-T. Yeh, Catal. Today 148 (2009) 124–129.
[35] L. Mo, X. Zhang, C.-T. Yeh, Chem. Commun. (2004) 1426–1427.
[36] A. Nagy, G. Mestl, Appl. Catal., A: Gen. 188 (1999) 337–353.
[37] M. Turco, G. Bagnasco, U. Costantino, F. Marmottini, T. Montanari, G. Ramis, G. Busca, J. Catal. 228 (2004) 56–65.
[38] S. Sitshebo, A. Tsolakis, K. Theinnoi, Int. J. Hydrogen Energy 34 (2009) 7842–7850.
[39] T. Miyadera, Appl. Catal., B: Environ. 2 (1993) 199–205.
[40] T. Miyadera, K. Yoshida, Chem. Lett. 148 (1993) 3–1486.
[41] S. Kameoka, Y. Ukisu, T. Miyadera, Phys. Chem. Chem. Phys. 2 (2000) 367–372.
[42] J.H. Lee, S.J. Schmieg, S.H. Oh, Appl. Catal., A: Gen. 342 (2008) 78–86.
[43] H. Dong, S. Shuai, R. Li, J. Wang, X. Shi, H. He, Chem. Eng. J. 135 (2008) 195–201.
[44] C. Zhang, H. He, S. Shuai, J. Wang, Environ. Pollut. 147 (2007) 415–421.
[45] K. Shimizu, M. Tsuzuki, A. Satsuma, Appl. Catal., B: Environ. 71 (2007) 80–84.
[46] K. Arve, K. Eränen, M. Snåre, F. Klingstedt, D. Murzin, Top. Catal. 42–43 (2007) 399–403.
[47] M.K. Kim, P.S. Kim, J.H. Baik, I.-S. Nam, B.K. Cho, S.H. Oh, Appl. Catal., B: Environ. 105 (2011) 1–14.
[48] X. Shi, Y. Yu, H. He, S. Shuai, H. Dong, R. Li, J. Environ. Sci. 20 (2008) 177–182.
[49] M. Männikkö, M. Skoglundh, H.H. Ingelsten, Appl. Catal., B: Environ. 119–120 (2012) 256–266.
[50] M. Männikkö, M. Skoglundh, H. Härelind, Top. Catal. 56 (2013) 145–150.
[51] Y. Yu, H. He, Q. Feng, J. Phys. Chem. B 107 (2003) 13090–13092.
[52] Y. Yu, H. He, Q. Feng, H. Gao, X. Yang, Appl. Catal., B: Environ. 49 (2004) 159–171.
[53] Y.H. Yeom, M. Li, W.M.H. Sachtler, E. Weitz, J. Catal. 238 (2006) 100–110.
[54] T.B. Reed, R.M. Lerner, Science 182 (1973) 1299–1304.
[55] A.S. Moffatt, Science 251 (1991) 514–515.
[56] R.H. Williams, E.D. Larson, R.E. Katofsky, J. Chen, Energy Sustainable Dev. 1 (1995) 18–34.
[57] R.J. Nichols, J. Sci. Ind. Res. 62 (2003) 97–105.
[58] K. Kumabe, S. Fujimoto, T. Yanagida, M. Ogata, T. Fukada, A. Yabe, T. Minowa, Fuel 87 (2008) 1422–1427.
[59] Z. Fan, Z. Xia, S. Shijin, X. Jianhua, W. Jianxin, Energy Fuels 24 (2010) 1283–1292.
[60] J.V. Larsen, B.T. Dalslet, A.-C. Johansson, C. Kallesøe, E.V. Thomsen, J. Power Sources 257 (2014) 237–245.
[61] Y.W. Zhang, G.H. Chang, S. Liu, J.Q. Tian, L. Wang, W.B. Lu, X.Y. Qin, X.P. Sun, Catal. Sci. Technol. 1 (2011) 1636–1640.
[62] K. Eränen, F. Klingstedt, K. Arve, L.-E. Lindfors, D.Y. Murzin, J. Catal. 227 (2004) 328–343.
[63] P. Sazama, L. Čapek, H. Drobná, Z. Sobalík, J. Dědeček, K. Arve, B. Wichterlová, J. Catal. 232 (2005) 302–317.
[64] F.C. Meunier, J.P. Breen, V. Zuzaniuk, M. Olsson, J.R.H. Ross, J. Catal. 187 (1999) 493–505.
[65] N. Bion, J. Saussey, M. Haneda, M. Daturi, J. Catal. 217 (2003) 47–58.
[66] S. Tamm, H.H. Ingelsten, A.E.C. Palmqvist, J. Catal. 255 (2008) 304–312.
[67] S. Tamm, H.H. Ingelsten, M. Skoglundh, A.E.C. Palmqvist, J. Catal. 276 (2010) 402–411.